new diagnostic for the study of channel formation, which has relevance to any application requiring extended propagation of intense laser beams. Although these measurements are time-integrated, it is expected that the electrons are accelerated in microbunches that are a fraction of the plasma period (23 fs) in duration, separated by a plasma period, and in a macrobunch duration that is less than the laser pulse duration (400 fs).

REFERENCES AND NOTES

1. C. Max, J. Arons, A. B. Langdon, *Phys. Rev. Lett.* **33**, 209 (1974).
2. P. Mora and T. M. Antonsen Jr., *Phys. Rev. E* **53**, R2068 (1996).
3. G. Z. Sun, E. Ott, Y. C. Lee, P. Guzdar, *Phys. Fluids* **30**, 526 (1987).
4. A. B. Borisov *et al.*, *Phys. Rev. A* **45**, 5830 (1992).
5. D. C. Barnes, T. Kurki-Suonio, T. Tajima, *IEEE Trans. Plasma Phys.* **PS-15**, 154 (1987).
6. P. Maine *et al.*, *IEEE J. Quantum Electron.* **24**, 398 (1988); G. Mourou and D. Umstadter, *Phys. Fluids B* **4**, 2315 (1992).
7. T. Tajima and J. M. Dawson, *Phys. Rev. Lett.* **43**, 267 (1979).
8. P. Sprangle, E. Esarey, J. Krall, G. Joyce, *ibid.* **69**, 2200 (1992).
9. T. M. Antonsen Jr. and P. Mora, *ibid.*, p. 2204.
10. N. E. Andreev, L. M. Gorbunov, V. I. Kirsanov, A. Pogosova, R. R. Ramazashvili, *Pis'ma Zh. Eksp. Teor. Fiz.* **55**, 551 (1992) [*JETP Lett.* **55**, 571 (1992)].
11. J. Krall, A. Ting, E. Esarey, P. Sprangle, G. Joyce, *Phys. Rev. E* **48**, 2157 (1993).
12. E. Esarey, J. Krall, P. Sprangle, *Phys. Rev. Lett.* **72**, 2887 (1994).
13. C. Decker, W. B. Mori, T. Katsouleas, *Phys. Rev. E* **50**, R3338 (1994); W. B. Mori *et al.*, *Phys. Rev. Lett.* **72**, 1482 (1994).
14. S. V. Bulanov, F. Pegoraro, A. M. Pukhov, *Phys. Rev. Lett.* **74**, 710 (1995).
15. S. C. Wilks, W. L. Kruer, E. A. Williams, P. Amendt, D. C. Eder, *Phys. Plasmas* **2**, 274 (1995).
16. A. I. Akhiezer and R. V. Polovin, *Sov. Phys. JETP* **3**, 696 (1956).
17. C. A. Coverdale *et al.*, *Phys. Rev. Lett.* **74**, 4659 (1995).
18. A. J. Mackinnon *et al.*, *ibid.* **76**, 1473 (1996).
19. The EPW amplitude was estimated with the standard Bragg scattering equation, $P_s/P_0 \sim (\Delta n/n_e)^2(n_e/n_c)^2(V/2z_r\lambda^2)$, where V is the volume the plasma wave occupies [R. E. Slusher and C. M. Surko, *Phys. Fluids* **23**, 472 (1980)]. This result was consistent with a numerical simulation that simply allows a laser pulse to undergo a Fourier transform. This laser pulse is then phase-modulated by a copropagating plasma wave and oscillating background electrons such that $I(t) = I_0(t)\exp[-i(2\pi/\lambda)\Delta n(t)L]$, where $\Delta n(t) = -[\omega_{p0}^2/2\omega^2\gamma(t)][1 + (\tilde{n}/n_e)\cos W_p(t)t]$ is the change of refractive index and $I_0(t)$ is the initial laser pulse intensity.
20. Equation 3 predicts an amplitude of $\tilde{n}/n_e \sim 5$ to 40% (which corresponds to 9.4 to 11.6 e foldings) for 0.6 TW to 1 TW, assuming growth from an initial noise level predicted by theory (*21*), 4×10^{-6}, and a propagation distance $z/z_R = 1.0$, limited by refraction; the latter quantities have not actually been measured.
21. K.-C. Tzeng, W. B. Mori, C. D. Decker, *Phys. Rev. Lett.* **76**, 3332 (1996).
22. A. Modena *et al.*, *Nature* **377**, 606 (1995).
23. K. Nakajima *et al.*, *Phys. Rev. Lett.* **74**, 4428 (1995).
24. A. Pukhov and J. Meyer-ter-Vehn, *ibid.* **76**, 3975 (1996).

25. We would like to thank P. Bucksbaum, M. Downer, R. Gilgenbach, D. Gustafson, L. Jones, Y. Y. Lau, P. Le Blanc, X. Liu, and B. Roe for many useful discussions. Financial support was provided by the National Science Foundation and the U.S. Department of Energy.

2 February 1996; accepted 8 May 1996

Rates of DNA-Mediated Electron Transfer Between Metallointercalators

M. R. Arkin, E. D. A. Stemp, R. E. Holmlin, J. K. Barton,* A. Hörmann, E. J. C. Olson, P. F. Barbara*

Ultrafast emission and absorption spectroscopies were used to measure the kinetics of DNA-mediated electron transfer reactions between metal complexes intercalated into DNA. In the presence of rhodium(III) acceptor, a substantial fraction of photoexcited donor exhibits fast oxidative quenching ($>3 \times 10^{10}$ per second). Transient-absorption experiments indicate that, for a series of donors, the majority of back electron transfer is also very fast ($\sim 10^{10}$ per second). This rate is independent of the loading of acceptors on the helix, but is sensitive to sequence and π stacking. The cooperative binding of donor and acceptor is considered unlikely on the basis of structural models and DNA photocleavage studies of binding. These data show that the DNA double helix differs significantly from proteins as a bridge for electron transfer.

Many researchers have considered whether the aromatic heterocyclic bases in duplex DNA offer a medium for fast, long-range electron transfer (ET) (*1–10*). Intercalated electron donors and acceptors provide a direct probe of the DNA π stack. Subnanosecond luminescence quenching of photoexcited Ru(II) donors by Rh(III) acceptors occurs when both complexes are intercalatively stacked into B-form DNA (B-DNA), but fast quenching is not observed with a nonintercalating acceptor in a reaction with comparable driving force (*3*, *4*). Indeed, with metallointercalators covalently attached to a 15–base pair (bp) DNA duplex and separated by >40 Å, a lower limit on the intramolecular quenching was set at $\sim 3 \times 10^9$ s^{-1} (*4*). Here we have used ultrafast emission and absorption spectroscopies to examine fast ET reactions mediated by DNA with a series of noncovalently bound, intercalated metal complexes.

The photoexcited donors (Fig. 1) display large enhancements of luminescence upon DNA intercalation (*11–13*). Two-dimensional nuclear magnetic resonance (NMR) studies show that the dppz ligand of $Ru(phen)_2dppz^{2+}$ (phen, 1,10-phenanthroline; dppz, dipyridophenazine) intercalates into B-DNA from the major groove (*14*) with a binding constant of $>10^7$ M^{-1} (*15*). For $M(phen)_2dppz^{2+}$ derivatives (M = Ru, Os), the lowest energy electronic transition is characterized by metal-to-ligand charge transfer (MLCT) directed onto the dppz ligand (*13*, *16*). In aqueous solutions, the excited state of these complexes is quenched by proton transfer from water to the phenazine N atoms (*12*, *13*); when the dppz ligand is protected from water by DNA intercalation, this pathway is inhibited, and emission typical of these polypyridyl complexes is detected. Hence, excitation of the complexes bound to DNA promotes an electron onto the intercalating ligand, directing it into the π stack.

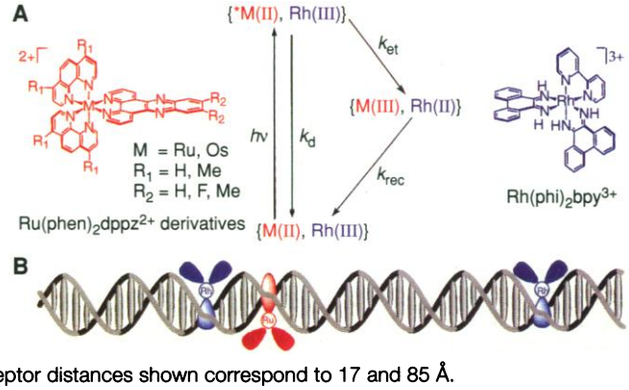

Fig. 1. (**A**) Intercalating donors (M = Ru, Os) and acceptor Rh(III) and the ET cycle. Photoexcitation of M(II) forms the excited state *M(II), which can radiatively decay (k_d) or can be quenched by ET with Rh(III) (k_{et}) to form M(III)-Rh(II) and then recombine (k_{rec}). Photoinduced ET may yield either Rh(II)(phi)$_2$bpy or Rh(III)(phi)(phi$^-$)bpy, both symbolized as Rh(II). (**B**) Ru and Rh bound to DNA at typical ratios used in these experiments; the donor-acceptor distances shown correspond to 17 and 85 Å.

M. R. Arkin, E. D. A. Stemp, R. E. Holmlin, J. K. Barton, Beckman Institute, California Institute of Technology, Pasadena, CA 91125, USA.
A. Hörmann, E. J. C. Olson, P. F. Barbara, Department of Chemistry, University of Minnesota, Minneapolis, MN 55455, USA.
*To whom correspondence should be addressed.

In aqueous buffer, in the absence of DNA, the photoexcited donors show no steady-state luminescence and have excited-state lifetimes from 85 to 500 ps for Ru and 10 to 30 ps for Os (Table 1). Therefore, DNA intercalation increases the excited-state lifetime of these complexes by three orders of magnitude. Ultrafast time-correlated single photon counting (TCSPC) confirms the kinetics observed by transient absorption spectroscopy (*17*).

We used $Rh(phi)_2bpy^{3+}$ (phi, 9,10-phenanthrenequinone diimine; bpy, 2,2′-bipyridine) as the electron acceptor (Fig. 1). NMR studies have shown that phi complexes of Rh(III) intercalate into B-DNA from the major groove (*18*). Irradiation of the bound Rh(III) complex with ultraviolet light leads to direct strand scission of the DNA at the site of phi intercalation (*19*); by this photocleavage assay, $Rh(phi)_2bpy^{3+}$ binds in a sequence-neutral manner (binding constant $K_b \approx 10^7\ M^{-1}$) (*20*).

We examined the photoinduced forward (k_{et}) and recombination (k_{rec}) ET reactions on the picosecond time scale by monitoring both the kinetics of the emission decay and the kinetics of the recovery in ground-state absorption by Ru(II) and Os(II) donors (*21*) (Fig. 1). All experiments were done at a ratio of 50 DNA base pairs to one electron donor, such that the complexes are dilute on the helix.

Figure 2 shows experimental data for Δ = $Ru(phen)_2dpp_3^{2+}$ bound to DNA quenched by Δ = $Rh(phi)_2bpy^{3+}$. Emission quenching of $Ru(phen)_2dppz^{2+}$ by $Rh(phi)_2phen^{3+}$ is too fast to be resolved by nanosecond flash photolysis instrumentation (*3*). Similarly, when quenching of *Ru(II) by $Rh(phi)_2bpy^{3+}$ is measured by either flash photolysis or TCSPC on the picosecond time scale, no change in the emission kinetics is observed; instead, there is a large decrease in the emission intensity at zero time (Fig. 2A). This loss of intensity implies that emission quenching occurs faster than our time resolution, so we assign a lower limit of $\sim 3 \times 10^{10}\ s^{-1}$ to k_{et} on the basis of the resolution of the TCSPC apparatus. As the concentration of Rh bound to DNA is increased, a corresponding decrease in the initial intensity is observed.

We quantified the fraction of excited states undergoing ET with $k_{et} > 3 \times 10^{10}\ s^{-1}$ by comparing data obtained by two different techniques (Fig. 2B). We used laser flash photolysis to measure steady-state luminescence by integrating the full emission decay curve. Total quenching is then given by a comparison of luminescence in

Table 1. Excited-state lifetimes of photoexcited electron donors in the absence and presence of DNA. F_2-dppz, 7,8-difluoro dipyridophenazine; Me_2-dppz, 7,8-dimethyl dipyridophenazine; DMP, 4,7-dimethyl-1,10 phenanthroline. Transient absorption data for donors without DNA were taken with λ_{exc} = 400 nm and λ_{obs} = 420 nm. Samples contained 40 μM complex in 5 mM tris and 50 mM NaCl (pH 8.5). Error in lifetimes is estimated to be ≤15%. For donors bound to DNA, luminescence decay data were taken with λ_{exc} = 480 nm and λ_{obs} = 616 nm. Samples contained 10 μM metal complex, 500 μM bp calf thymus DNA. Error in lifetimes is estimated to be ±10%. The percentages indicate the magnitude of the preexponential factor in a biexponential fit; for transient absorption, there is a small residual offset.

Donor	− DNA		+ DNA	
	τ (ns)	%	τ (ns)*	%
Δ-$Ru(phen)_2dppz^{2+}$	0.25	97	160	80
			850	20
Λ-$Ru(phen)_2dppz^{2+}$			40	85
			150	15
rac-$Ru(bpy)_2dppz^{2+}$	0.21	95	100	90
			450	10
Δ-$Ru(DMP)_2dppz^{2+}$	0.11	96	30	80
			125	20
Δ-$Ru(phen)_2(F_2\text{-dppz})^{2+}$			40	85
			280	15
rac-$Ru(phen)_2(Me_2\text{-dppz})^{2+}$	0.085	8†	370	65
	0.49	50	1170	35
Δ-$Os(phen)_2dppz^{2+}$	0.0096	60†	1.5	75
	0.026	33	9.2	25
Δ-$Ru(phen)_2dppz^{2+}$, D_2O	0.56	96	400	75
			1240	25

*The two excited-state decays for bound species have been ascribed to two orientations of the intercalated dppz ligand within the base stack, which vary in their accessibility to solvent (*11–14*). The excited-state lifetimes of Δ- and Λ-$Ru(phen)_2dppz^{2+}$ in the presence of DNA are sensitive to the metal/DNA ratio (*15*). †The observed biexponential decays probably reflect competing pathways for excited-state decay.

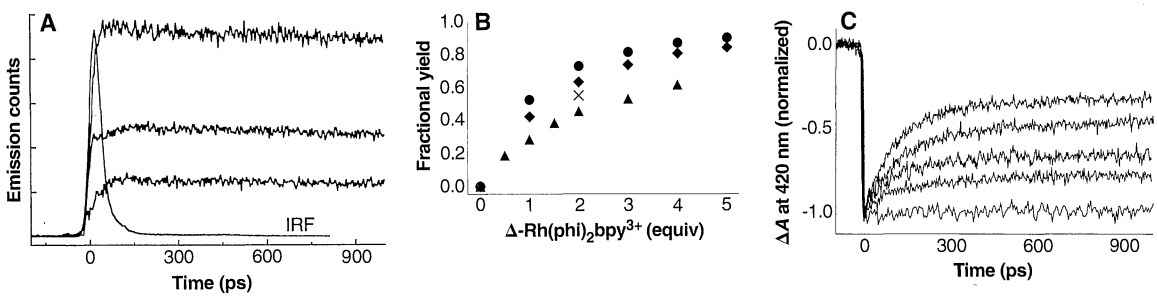

Fig. 2. (**A**) Time-resolved emission decays measured by TCSPC for Δ-*Ru in the presence of (top to bottom) 0, 1, and 2 equiv of Δ-Rh, illustrating the large amount of quenching occurring with $k_{et} > 3 \times 10^{10}\ s^{-1}$. Data have been corrected for a response-limited emission decay of $Rh(phi)_2bpy^{3+}$. IRF, instrument response function. (**B**) Fractional yields of the forward and back ET reactions: (●) steady-state (total) quenching, determined by nanosecond laser flash photolysis, (◆) quenching occurring with $k_{et} > 10^8\ s^{-1}$, also measured by nanosecond laser flash photolysis, (×) quenching occurring with $k_{et} > 3 \times 10^{10}\ s^{-1}$, determined by picosecond TCSPC, and (▲) absorption recovery, occurring with $k_{rec} = 9 \times 10^9\ s^{-1}$. (**C**) Time-resolved transient absorption data monitoring the ground-state recovery kinetics of Δ-$Ru(phen)_2dppz^{2+}$ bound to DNA as a function of Δ-$Rh(phi)_2bpy^{3+}$ concentration: (bottom to top) 0, 0.5, 1, 2, and 4 equiv Δ-Rh(III). Data are corrected for a small contribution from *Rh(III) and are normalized with respect to the change in absorbance (Δ*A*) at time zero. Steady-state luminescence intensities were determined by integrating the full emission decay curves obtained in nanosecond flash photolysis experiments with λ_{exc} = 480 nm and λ_{obs} = 616 nm. The amount of ultrafast quenching by Rh(III) is revealed by the prompt loss in initial intensity of emission decay curves measured by flash photolysis and TCSPC (λ_{exc} = 400 nm, λ_{obs} = 620 nm). Transient absorption data are measured with λ_{exc} = 390 nm and λ_{obs} = 420 nm and are fit to a biexponential decay, where a slow kinetic component is used to describe the offset. The absolute concentrations of reagents do not affect the quenching rates nor the amount of quenching, but are typically 10 μM Ru-Os for the emission decay experiments and 20 μM Ru-Os for transient absorption measurements. Sonicated calf thymus DNA (Pharmacia), with an average length of 2000 ± 600 bp, was used at a ratio of one M(II) to 50 bp. All experiments were conducted in an aerated buffer of 5 mM tris and 50 mM NaCl, pH 8.5 at ambient temperature.

the presence and absence of acceptor; the fraction of emission quenching that occurs faster than the 10-ns response of this instrument is revealed by the loss of initial intensity at zero time. Picosecond TCSPC revealed initial intensity losses comparable to those obtained by laser flash photolysis, and no additional kinetic components were observed. The prompt loss of initial intensity measured by flash photolysis and TCSPC indicates that most of the quenching occurs with $k_{et} > 3 \times 10^{10}$ s^{-1}. Because a small amount of reaction occurs on a time scale longer than 10 ns, there is a discontinuous distribution of photoinduced ET rates, composed of a substantial ultrafast component (with $k_{et} > 3 \times 10^{10}$ s^{-1}) and a smaller population with $k_{et} < 10^8$ s^{-1}.

Picosecond transient absorption spectroscopy was used to follow the recovery of the Ru(II) or Os(II) ground-state absorption at 420 nm (Fig. 2C). In the absence of quencher, the ground-state absorption recovers on a time scale longer than 3 ns for *Ru(II) bound to DNA, consistent with the excited-state lifetimes of >150 ns. As Δ-Rh(phi)$_2$bpy^{3+} is added to Δ-Ru(phen)$_2$dppz^{2+} bound to DNA, a fast component with $k \sim 10^{10}$ s^{-1} is evident in the kinetics of ground-state recovery (*22*). The amplitude of this kinetic component increases substantially with increasing Δ-Rh(III) concentration. A bleach in this absorption band of MLCT could indicate the presence of either excited-state donor or oxidized donor, or both. The TCSPC measurements, however, revealed that no quenching occurs with a rate constant of 10^{10} s^{-1} and that $k_{et} > 3 \times 10^{10}$ s^{-1} for the major component, so the dynamics measured here by transient absorption spectroscopy correspond to decay of an ET intermediate; that is, Ru(III) + Rh(II) → Ru(II) + Rh(III). These data combined with other spectroscopic studies establish that quenching occurs by electron transfer (*23, 24*).

Not all of the donor population quenched with high k_{et} undergoes fast ($k_{rec} = 9 \times 10^9$ s^{-1}) back ET, because the fraction of fast absorption recovery is always less than the fraction of ultrafast emission quenching (Fig. 2B). For example, at 1 equivalent (equiv) Δ-Rh, the fraction of ultrafast quenching is 0.42, whereas the fraction of fast recombination is 0.28; therefore, 67% of the Ru(III)-Rh(II) intermediates react with $k_{rec} = 9 \times 10^9$ s^{-1}. No intermediate persists beyond the excited-state decay of unquenched Δ-*Ru(phen)$_2$dppz^{2+} (time > 2 μs); thus, the remaining 33% of intermediates react with 10^9 s$^{-1} > k_{rec} > 10^6$ s^{-1}. It is technically difficult to measure the recombination kinetics in this time window owing to interfering, spectrally similar signals from *M(II). For two other donors, however, transient intermediates have been observed on the microsecond time scale (*23, 24*), and these long-lived ET products might also be generated in the ultrafast quenching process. Because recombination occurs on picosecond to microsecond time scales, the distribution of rates is wider for the recombination reaction than for the quenching reaction (*25*).

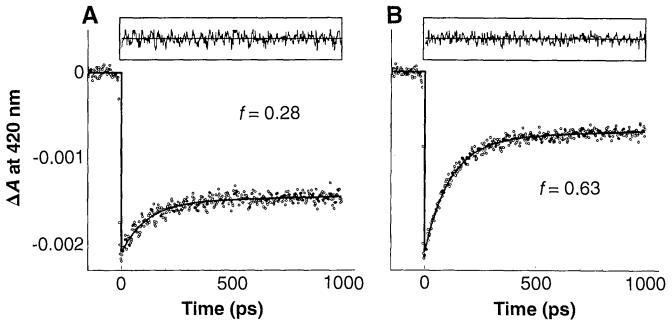

Fig. 3. Recovery of ground-state absorption after photoexcitation for Δ-Ru(phen)$_2$dppz^{2+} bound to DNA in the presence of (**A**) 1 equiv and (**B**) 4 equiv of Δ-Rh(phi)$_2$bpy^{3+}. The plots show transient absorption data fit to $\Delta A(t) = \Delta A(0)\,[f\exp(-k_1 t) + (1-f)\exp(-k_2 t)]$; fit residuals are displayed above the data. For the fits shown here, $f = 0.28$ and $k_2 = 4.0 \times 10^7$ s^{-1} for 1 equiv of acceptor, and $f = 0.63$ and $k_2 = 1.2 \times 10^8$ s^{-1} for 4 equiv of acceptor; k_1 ($= k_{rec}$) was fixed at 8.7×10^9 s^{-1} in both cases. When it is not fixed, k_1 remains constant (±15%) for each point in the titration. The signals are well-described by a single fast rate constant and a second, slower decay; fitting the data to a single-exponential function with an offset gives equivalent results. Conditions are as given in Fig. 2.

Regardless of whether the average loading of metal complexes is 1 in 33 bp or 1 in 10 bp, the fast dynamics exhibited by Δ-Ru(phen)$_2$dppz^{3+} are well described under all conditions by an exponential decay of 9.0×10^9 s^{-1} (Fig. 3). Because ET rates typically decay exponentially with distance [$k \propto e^{-\beta R}$, where β is the decay coupling parameter and R is distance (*26*)], a single rate suggests either that ET occurs over only one distance or a shallow dependence of the rate.

The reactivity of seven donor-acceptor pairs in mixed-sequence DNA was investigated (Table 2); the donors varied with respect to shape, hydrophobicity, and photophysical properties. The rate constant for the fast component of bleach decay was independent of the donor-acceptor ratio, and the fraction of this fast component increased concomitantly with the amount of emission quenching, as observed by emission measurements. The most significant change in driving force is with Os(phen)$_2$dppz^{2+} (~500 mV), but this decrease has only a small effect on k_{rec}. Δ-Os(phen)$_2$dppz^{2+} followed a quenching profile (*24*) similar to that of its isostructural Ru(II) analog and had $k_{et} > 3 \times 10^{10}$ s^{-1}, but it exhibited a slightly faster k_{rec} (1.1×10^{10} s^{-1}) than did Ru(III) (*27, 28*). Interestingly, more Os(III) recombines with Rh(II) on the picosecond time scale than does Ru(III). The results with Os(phen)$_2$dppz^{2+} also show that an insensitivity of k_{rec} to loading still occurs when there is not a large difference between the intrinsic rate of excited-state decay and the rate of recombination.

The efficiency of emission quenching and the rate of back ET are both sensitive to stacking of the electron donor in DNA (Table 2), as illustrated by Λ- and Δ-Ru(phen)$_2$dppz^{2+}. Table 2 shows that Δ-Ru(phen)$_2$dppz^{2+} is quenched by Δ-Rh(phi)$_2$bpy^{3+} (3 equiv) bound to DNA twice as effectively as is Λ-Ru(phen)$_2$dppz^{2+}

Table 2. ET quenching and ground-state recombination (rec) of photoexcited electron donors bound to DNA with Δ-Rh(phi)$_2$bpy^{3+} as the electron acceptor. The $\%_{quench}$ represents the amount of total quenching at 3 equiv of Δ-Rh(phi)$_2$bpy^{3+}. The $\%_{rec}$ values are the fraction of fast ground-state recovery at 3 equiv of Δ-Rh(phi)$_2$bpy^{3+}, as determined by the preexponential factors of a biexponential fit. Error in rates is estimated as <15% and in percentages as <5%. Reaction driving force ΔG° for quenching and recombination reactions are calculated from reduction potentials determined by cyclic voltammetry (DMF, 100 mV s^{-1}). Ratio of DNA bp/donor = 50. Other conditions are as in Fig. 2. λ_{obs} = 73% nm for Os(II) emission.

Donor	k_{rec} (10^9 s^{-1})	$\%_{quench}$	$\%_{rec}$	$-\Delta G^\circ_{quench}$ (V)	$-\Delta G^\circ_{rec}$ (V)
Δ - Ru(phen)$_2$dppz^{2+}	9.2	82	53	0.56	1.66
rac-Ru(bpy)$_2$dppz^{2+}	7.1	68	60*	0.52	1.69
Δ - Ru(DMP)$_2$dppz^{2+}	11	47	44	0.59	1.59
Δ - Ru(phen)$_2$(F$_2$-dppz)$^{2+}$	7.7	81	47	0.54	1.68
rac-Ru(phen)$_2$(Me$_2$-dppz)$^{2+}$	8.3	82	44	0.57	1.67
Δ - Os(phen)$_2$dppz^{2+}	11	80	64	0.73	1.21
Λ-Ru(phen)$_2$dppz^{2+}	4.5	43	20		

*Ratio of DNA bp/donor = 25.

(*29*), although both donors are fully bound and the two reactions have the same driving force (*30*). Also, k_{rec} is 9×10^9 s^{-1} for Δ-Ru(phen)$_2$dppz^{2+} but only 5×10^9 s^{-1} for the Λ isomer. The lifetimes for the Δ isomer bound to DNA are more than twice those observed for Λ-Ru(phen)$_2$dppz^{2+} (Table 1), indicating that water is less accessible to the right-handed intercalator. Thus, the excited-state lifetimes of the Λ versus the Δ isomer in the absence of quencher correlate with the closer stacking of the right-handed Δ enantiomer within the right-handed DNA helix (*31*). Thus, the more deeply stacked enantiomer was more efficiently quenched and showed faster recombination kinetics. In general, there is a correlation between the length of excited-state lifetimes and the efficiency of ultrafast quenching (Table 2), supporting the idea that deeper stacking facilitates ET.

Electron transfer is mediated by the DNA helix. The rate of ground-state recovery of DNA-bound Δ-Ru(phen)$_2$dppz^{2+} in the presence of Rh ($k_{rec} \approx 1 \times 10^{10}$ s^{-1}) was more than twice that of Ru(phen)$_2$dppz^{2+} in water ($k_d \approx 4 \times 10^9$ s^{-1}) without DNA (Table 1). This result argues against displacement of intercalated Ru(II) complexes by Rh(III) complexes, where the excited state would simply be quenched by water outside of the DNA. Moreover, no solvent-isotope effect is seen in quenching titrations with Rh(III) (*32*) or the kinetics of back ET, whereas a significant isotope effect has been observed for quenching of Ru(II) in both acetonitrile and DNA ($k_H/k_D \approx 2.2$) (*12, 32*). Thus, water does not directly participate in the ET reaction.

The photocleavage assay developed for phi complexes of Rh(III) was used to determine the effect of the various Ru(II) donors on the binding of Δ-Rh(phi)$_2$bpy^{3+} (*33, 34*) (Fig. 4). The rhodium complex cleaved a 180-bp DNA restriction fragment at each base pair site, but not with uniform intensity. We expect the sequence selectivity of dppz complexes of Ru(II) also to be fairly low (*12, 14*). Nonetheless, if Ru(II) and Rh(III) complexes bound cooperatively on the DNA, cleavage by Rh(III) at its preferred sites would become still more intense in the presence of Ru(II). The characteristic cleavage pattern is unchanged, however, in the presence of Δ-Ru(phen)$_2$dppz^{2+} or *rac*-Ru(bpy)$_2$dppz^{2+} (Fig. 4), indicating that neither complex perturbs the binding of Δ-Rh(phi)$_2$bpy^{3+} under these conditions (*35*).

Titrations were also carried out with poly[d(AT)] and poly[d(GC)] to determine the effect of sequence. Transient bleach decays of Δ-Ru(phen)$_2$dppz^{2+} bound to poly[d(AT)] in the presence of Δ-Rh(phi)$_2$bpy^{3+} (Fig. 5) show that the kinetics were largely unchanged ($k_{rec} = 7 \times 10^9$ s^{-1}) compared with those of mixed-sequence DNA, but the amount of emission quenching was greater for the alternating d(AT) polymer. In poly[d(GC)], however, k_{rec} is much reduced (2×10^8 s^{-1}), and emission quenching is less efficient (16% versus 70% for poly[d(AT)] at 1 equiv of Rh). Baguley and co-workers (*5*) have also observed more efficient ET quenching in poly[d(AT)] than in poly[d(GC)] in their studies with ethidium bromide and amsacrine.

This sensitivity to sequence further indicates that ET proceeds through the DNA (*36*) and is not a function of van der Waals contact between bound intercalators; even at the nearest available intercalation site, the interaction distance through DNA is 10.2 Å, the neighbor-excluded distance (*37*). Both alternating polymers are B-form, although poly[d(AT)] is considered more flexible (*38*). From the photocleavage study, the Rh(III) complex binds to all DNA sites with little preference for AT- or GC-rich regions. Hence, neither the integrity of the DNA duplex nor the binding affinity of the metal complexes can account for the difference in quenching rates.

The insensitivity of back ET rates to loading of Rh(III) intercalators on DNA is noteworthy. For random binding of the Ru(II) and Rh(III) complexes, 2% of the Ru-Rh distances are nearest neighbors at 0.5 equiv of Rh, yet 20% of Δ-Ru show rapid ground-state recovery at this loading in mixed-sequence DNA. Similarly, 16% of Ru-Rh pairs are in closest contact at 4 equiv of Rh, where 60% of molecules return to the ground state with $k_{rec} = 9 \times 10^9$ s^{-1}. The fast quenching of *M(II) is also likely simple first order at times <10 ns. If the early ET kinetics were not first order and the rates decayed with an exponential distance dependence, we should have observed some slower components (10^{10} to 10^8 s^{-1}). Thus, neither the quenching nor the transient absorption data are consistent with ET over discrete, multiple distances related by an exponential decay with distance.

To account for the insensitivity of the rate of recombination to loading, we considered two possibilities: clustering of donors and acceptors on the helix and distance-independent ET over a finite distance. A cooperative donor-acceptor binding model leading to a high concentration of nearest-neighbor pairs could account for the observation of simple first-order kinetics in the transient absorption data, but the model

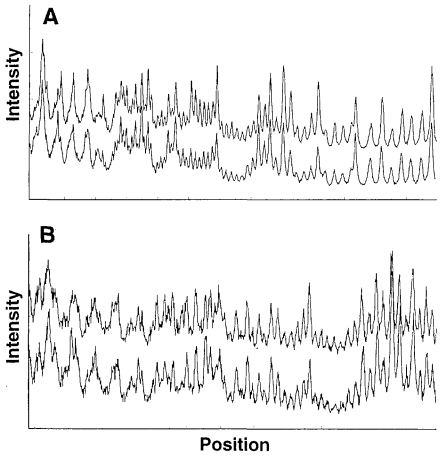

Fig. 4. Gel electrophoresis measurements of DNA photocleavage by Δ-Rh(phi)$_2$bpy^{3+}. Shown are phosphorimager scans of a 180-bp, [3′-^{32}P]-end-labeled DNA restriction fragment from pUC18 (Eco RI–PVU II). (**A**) Photocleavage of 180-bp fragment with 10 μM Δ-Rh(phi)$_2$bpy^{3+} irradiated at 313 nm for 7 min (*33*) in the presence (top) and absence (bottom) of 10 μM Δ-Ru(phen)$_2$dppz^{2+}. (**B**) Photocleavage of 180-bp fragment with 10 μM Δ-Rh(phi)$_2$bpy^{3+} in the presence (top) and absence (bottom) of 10 μM *rac*-Ru(bpy)$_2$dppz^{2+}. The two sets of histograms represent different regions of the same 180-bp sequence. Conditions are as given in Fig. 2 for photophysical measurements of ET. Data analyzed with ImageQuant software (Molecular Dynamics, Sunnyvale, California).

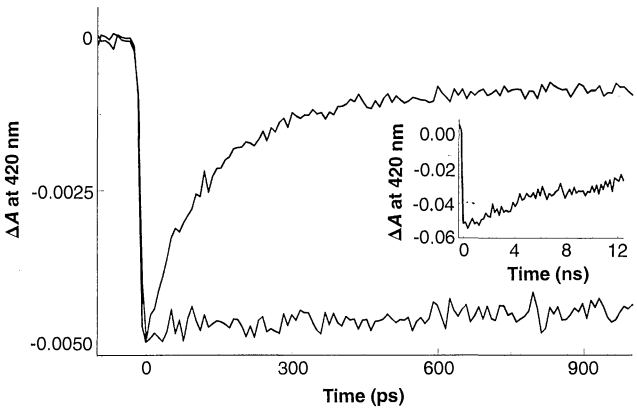

Fig. 5. Recovery of ground-state absorption of Δ-Ru(phen)$_2$dppz^{2+} bound to poly[d(AT)] (top trace) and poly[d(GC)] (bottom trace and inset) in the presence of Δ-Rh(phi)$_2$bpy^{3+}. For poly[d(AT)], $k_{rec} = 7 \times 10^9$ s^{-1} (70% at 3 equiv of Rh); for poly[d(GC)], $k_{rec} = 2 \times 10^8$ s^{-1} [47% at 4 equiv of Rh (*51*)]. The excited-state lifetimes for Δ-Ru(phen)$_2$dppz^{2+} in the absence of quencher are 120 ns (75%) and 720 ns (25%) in poly[d(AT)] and 37 ns (10%) and 280 ns (90%) in poly[d(GC)]. Conditions are as given in Fig. 2, except that average lengths of DNA are ~920 bp for poly[d(GC)] and ~1050 bp for poly[d(AT)] (Pharmacia).

would require a cooperative binding energy of 1.5 kcal mole^{-1} (39) to predict the efficiency of the ultrafast quenching process at low loading of Rh. Such highly cooperative binding of cationic metallointercalators on DNA has been observed thus far only for a phi complex of Rh(III) bearing phenyl substituents, which allow intermolecular contact of the ancillary ligands (40); by contrast, the ancillary ligands on the molecules used here do not permit a significant amount of π overlap or hydrophobic contact between adjacent molecules. Additionally, we have compared quenching in DNA and in SDS micelles (32), which are expected to encourage clustering (41), and found that fast quenching only occurs in the presence of DNA. Also, the photocleavage assay (Fig. 4) provides no evidence for cooperativity. Although a cooperative binding model cannot be definitively ruled out in an experiment with noncovalently bound donors and acceptors, these studies provide no evidence for such a phenomenon.

Without direct contact, an interaction resulting in one donor-acceptor distance is difficult to rationalize. Structural studies have shown that intercalation of similar Ru(II) and Rh(III) complexes cause only a local unwinding of the double helix (14, 18). The observed sequence dependence on ET indeed indicates that recombination does not involve reactants in direct van der Waals contact. Such direct contact could not explain the >30-fold difference in recombination rate observed for poly[d(GC)] and poly[d(AT)]. Even at closest approach, ET proceeds through the DNA over a nonbonded distance of 10.2 Å.

Alternatively, ET may be mediated by the DNA over some distance without a significant decrease in rate, rather than by a short-range interaction. A loading independence in k_{rec} is observed when the ancillary ligands, the intercalating ligand, the metal center, and even the chirality of the donor is varied. Furthermore, when the Ru(II) donor and Rh(III) acceptor were covalently bound and intercalated in a 15-bp oligonucleotide (4), where donor-acceptor separations were >40 Å, subnanosecond quenching was also observed. Similarly, long-range ET through DNA was evident in reactions where photoexcited $Rh(phi)_2bpy^{3+}$ oxidized guanine doublets over 34 Å (42). These results are consistent with the data described here, in which the rate of ET through the DNA duplex is fast, depends on stacking, and over some range of distances, is essentially independent of distance.

In contrast, the yields of both photoinduced ET and recombination do show a loading dependence, indicating that rapid long-range ET is precluded for some of the *M(II) population. Importantly, increasing the concentration of acceptor leads to an increase in the subnanosecond component of both the forward and reverse ET reactions. A plausible explanation is that reactants become isolated from one another beyond some critical separation (43); the fraction of quenching at low loadings suggests a reaction range of ~20 bp.

Our results therefore show that ET through DNA occurs on the picosecond time scale over a through-space distance of >10 Å at rates approaching those observed for initial charge separation in the photosynthetic reaction center (44). These results need to be understood in the context of theory and other experimental observations. Pathway calculations for ET by a superexchange mechanism (45) have been valuable in describing protein-mediated ET (with 0.8 Å^{-1} < $\beta \leq$ 1.4 Å^{-1}) (46). However, an analogy between DNA and σ-bonded pathways for ET could not explain the results obtained here unless one assumes a weak distance dependence (β < 0.2 Å^{-1}) for the π-stacked medium. The rate reported for an 8-bp oligonucleotide bearing metal complexes unstacked and coordinated to the sugar-phosphate backbone (8) could be understood by a pathway model in which the σ system limits access to the π stack. A hopping model in which the individual bridge elements are transiently oxidized or reduced has been useful in describing conductivity in stacked π systems in the solid state (10) and may be applicable to DNA as well (47). Other theories incorporate a small probability of thermal access of the electron to delocalized bridging states in the DNA (48), thus permitting ET through an adiabatic channel. More experimental data are needed before the distance dependence of ET through DNA will be well understood (49), and our work indicates that theoretical models must take into account the sensitivity of ET parameters to π-stacking interactions (7, 32, 50). Surely, the ET kinetics observed here paint an extraordinary picture for ET through DNA.

REFERENCES AND NOTES

1. For recent reviews, see M. R. Arkin, Y. Jenkins, C. J. Murphy, N. J. Turro, J. K. Barton, *Adv. Chem. Ser.* **246**, 449 (1995); E. D. A. Stemp and J. K. Barton, *Met. Ions Biol. Syst.* **33**, 325 (1996); T. J. Meade, *ibid.*, p. 453.
2. J. K. Barton, C. V. Kumar, N. J. Turro, *J. Am. Chem. Soc.* **108**, 6391 (1986); M. D. Purugganan, C. V. Kumar, N. J. Turro, J. K. Barton, *Science* **241**, 1645 (1988).
3. C. J. Murphy *et al.*, *Proc. Natl. Acad. Sci. U.S.A.* **91**, 5315 (1994).
4. C. J. Murphy *et al.*, *Science* **262**, 1025 (1993).
5. B. C. Baguley and M. Le Bret, *Biochemistry* **23**, 937 (1984); L. M. Davis, J. D. Harvey, B. C. Baguley, *Chem. Biol. Interactions* **62**, 45 (1987).
6. D. W. Whillans, *Biochim. Biophys. Acta* **414**, 193 (1975); P. Fromherz and B. Rieger, *J. Am. Chem. Soc.* **108**, 5361 (1986); S. J. Atherton and P. C. Beaumont, *J. Phys. Chem.* **91**, 3993 (1987); P. M. Cullis, J. D. McClymont, C. R. Symons, *J. Chem. Soc. Faraday Trans.* **86**, 591 (1990); C. Houée-Levin, M. Gardes-Albert, A. Rouscilles, C. Ferradini, B. Hickel, *Biochemistry* **30**, 8216 (1991); S. J. Atherton and P. C. Beaumont, *J. Phys. Chem.* **99**, 12025 (1995).
7. A. M. Brun and A. Harriman, *J. Am. Chem. Soc.* **114**, 3656 (1992); *ibid.* **116**, 10383 (1994).
8. T. J. Meade and J. F. Kayyem, *Angew. Chem. Int. Ed. Engl.* **34**, 352 (1995); S. M. Risser, D. N. Beratan, T. J. Meade, *J. Am. Chem. Soc.* **115**, 2508 (1993).
9. A. Szent-Gyorgyi, I. Isenberg, S. L. Baird Jr., *Proc. Natl. Acad. Sci. U.S.A.* **46**, 1444 (1960); R. S. Snart, *Biopolymers* **12**, 1493 (1973); C. T. O'Konski, P. Moser, M. Shirai, *Biopolym. Symp.* **1**, 479 (1964); J. M. Warman, M. P. de Haas, P. G. Schouten, in *Congress Proceedings*, vol. II of *Radiation Research: A 20th-Century Perspective*, W. C. Dewey, M. Edington, R. J. M. Fry, E. J. Hall, G. F. Witmore, Eds. (Academic Press, New York, 1992), pp. 93–98; L. P. Candeias and S. Steenken, *J. Am. Chem. Soc.* **115**, 2437 (1993).
10. For other π-stacked systems, see T. J. Marks, *Angew. Chem. Int. Ed. Engl.* **29**, 857 (1990); G. Quirion, M. Poirier, K. K. Liou, B. M. Hoffman, *Synth. Met.* **42**, 2653 (1991); D. Markovitz, H. Bengs, H. Ringsdorf, *J. Chem. Soc. Faraday Trans.* **88**, 1275 (1992); P. G. Schouten *et al.*, *J. Am. Chem. Soc.* **116**, 6880 (1994).
11. A. E. Friedman, J.-C. Chambron, J.-P. Sauvage, N. J. Turro, J. K. Barton, *J. Am. Chem. Soc.* **112**, 4960 (1990).
12. Y. Jenkins, A. E. Friedman, N. J. Turro, J. K. Barton, *Biochemistry* **31**, 10809 (1992); R. M. Hartshorn and J. K. Barton, *J. Am. Chem. Soc.* **114**, 5919 (1992); C. Turro, S. H. Bossmann, Y. Jenkins, J. K. Barton, N. J. Turro, *ibid.* **117**, 9026 (1995).
13. R. E. Holmlin and J. K. Barton, *Inorg. Chem.* **34**, 7 (1995).
14. C. M. Dupureur and J. K. Barton, *J. Am. Chem. Soc.* **116**, 10286 (1994).
15. C. Hiort, P. Lincoln, B. Norden, *ibid.* **115**, 3448 (1993).
16. J.-C. Chambron, J.-P. Sauvage, E. Amouyal, P. Koffi, *New J. Chem.* **9**, 527 (1985); E. Amouyal, A. Homsi, J.-C. Chambron, J.-P. Sauvage, *J. Chem. Soc. Dalton Trans.* **6**, 1841 (1990); C. Creutz, M. Chou, T. L. Netzel, M. Okumura, N. Sutin, *J. Am. Chem. Soc.* **102**, 1309 (1980).
17. TCSPC indicates that in water the emission maximum from the $Ru(phen)_2dppz^{2+}$ excited state is shifted to longer wavelengths by more than 250 nm relative to the luminescence in DNA and organic solvents (E. J. C. Olson *et al.*, unpublished results).
18. S. S. David and J. K. Barton, *J. Am. Chem. Soc.* **115**, 2984 (1993); J. G. Collins, T. P. Shields, J. K. Barton, *ibid.* **116**, 9840 (1994); T. P. Shields and J. K. Barton, *Biochemistry* **34**, 15037 (1995); *ibid.*, p. 15049; B. P. Hudson, C. M. Dupureur, J. K. Barton, *J. Am. Chem. Soc.* **117**, 9379 (1995); R. H. Terbrueggen and J. K. Barton, *Biochemistry* **34**, 8227 (1995).
19. A. Sitlani, E. C. Long, A. M. Pyle, J. K. Barton, *J. Am. Chem. Soc.* **114**, 2303 (1992).
20. K. Uchida, A. M. Pyle, T. Morii, J. K. Barton, *Nucleic Acids Res.* **17**, 10259 (1989).
21. Picosecond instrumentation is detailed in (27). Instrumentation for nanosecond laser flash photolysis has been described in A. E. Friedman, C. V. Kumar, N. J. Turro, J. K. Barton, *Nucleic Acids Res.* **19**, 2595 (1991).
22. Transient absorption data were equally well described by a single-exponential function with an offset and by a biexponential function where the offset is represented by a slow decay constant. More complex expressions incorporating multiple exponential terms or distributions did not improve the fits. The signal-to-noise ratio of the data does not allow one to distinguish between a single decay and a narrow distribution of rates centered at 10^{10} s^{-1}, but we see no evidence for kinetics other than this 10^{10} s^{-1} component for times less than 1 ns.
23. E. D. A. Stemp, M. R. Arkin, J. K. Barton, *J. Am. Chem. Soc.* **117**, 2375 (1995).
24. R. E. Holmlin, E. D. A. Stemp, J. K. Barton, *ibid.* **118**, 5236 (1996).

25. Transient absorption measurements on the microsecond time scale suggest that Rh(II), formed in the initial ET reaction, does not contribute significantly to the size of the transient absorption signal for the ground-state recovery of M(II) (M = Ru, Os). The amplitude of fast recovery of ground-state absorption is therefore related to the fraction of M(III) reacting to regenerate M(II).
26. R. A. Marcus and N. Sutin, *Biochim. Biophys. Acta* **811**, 265 (1985).
27. Supplementary information available (*28*). Provided are a description of the laser apparatus used for ultrafast measurements and time-resolved transient absorption data monitoring the recovery of ground-state absorption of Δ-$Os(phen)_2dppz^{2+}$ in the presence of DNA and Δ-$Rh(phi)_2bpy^{3+}$.
28. The material can be accessed on the World Wide Web at http://www.science-mag.org/science/feature/beyond/#arkin and can be ordered from AAAS (see any current masthead page for ordering information).
29. Data is also available as a figure on the Web (*28*).
30. The greater accessibility of water to the DNA-bound Λ enantiomer, as suggested by its shorter excited-state lifetimes, will have some effect on the reorganization energy.
31. J. K. Barton, *Science* **233**, 727 (1986).
32. M. R. Arkin, E. D. A. Stemp, C. Turro, N. J. Turro, J. K. Barton, *J. Am. Chem. Soc.* **118**, 2267 (1996).
33. C. S. Chow and J. K. Barton, *Methods Enzymol.* **212**, 219 (1992).
34. A. Sitlani and J. K. Barton, *Biochemistry* **33**, 12100 (1994).
35. The pattern of photocleavage changes somewhat upon the addition of salt, indicating that this assay is highly sensitive to small changes in DNA structure.
36. Guanine has the lowest oxidation potential of all the bases. Therefore, if the single rate reflected oxidation of a proximal base by the oxidized donor, one would expect that the rate would be faster in poly[d(GC)], but we observe the opposite trend. Moreover, the loading-independent rate of $k_{rec} = 1 \times 10^{10}$ s^{-1} is observed for $Os(phen)_2dppz^{3+}$, for which oxidation of guanine is precluded on thermodynamic grounds [T. W. Welch, A. H. Corbett, H. H. Thorp, *J. Phys. Chem.* **99**, 11757 (1995)].
37. D. M. Crothers, *Biopolymers* **6**, 575 (1968); D. E. V. Schmechel and D. M. Crothers, *ibid.* **10**, 465 (1971).
38. M. Vorlickova and J. Kypr, *J. Biomol. Struct. Dyn.* **3**, 67 (1985); C. A. Hunter, *J. Mol. Biol.* **230**, 1025 (1993); K. Yanagi, G. G. Privé, R. E. Dickerson, *ibid.* **217**, 201 (1991).
39. We modeled the intercalation of metal complexes by loading a one-dimensional lattice with two different intercalators to simulate the distribution of separations between donors and acceptors on the DNA. For the Δ-$Ru(phen)_2dppz^{2+}$–Δ-$Rh(phi)_2bpy^{3+}$ pair of reactants, experimental data on all time scales are reasonably well described by $\beta \sim 1.5$ $Å^{-1}$ (*26*) and a preference ratio of 13 favoring nearest-neighbor cooperative binding of donor and acceptor (A. Hörmann, E. J. C. Olson, P. F. Barbara, unpublished results).
40 A. Sitlani, C. M. Dupureur, J. K. Barton, *J. Am. Chem. Soc.* **115**, 12589 (1993).
41. S. J. Atherton *et al.*, *J. Phys. Chem.* **91**, 3137 (1987).
42. D. B. Hall, R. E. Holmlin, J. K. Barton, unpublished results.
43. The subpopulation of more slowly reacting donors could be decoupled from acceptors by defects in base stacking. The finite probability of encountering such a defect, arising from DNA structural polymorphism, should increase with increasing donor-acceptor separationseparation.
44. S. Kartha, R. Das, J. R. Norris, *Met. Ions Biol. Syst.* **27**, 323 (1991); S. G. Boxer, *Annu. Rev. Biophys. Biophys. Chem.* **19**, 267 (1990).
45. H. M. McConnell, *J. Chem. Phys.* **35**, 508 (1961); C. A. Naleway, L. A. Curtiss, J. R. Miller, *J. Phys. Chem.* **95**, 8434 (1991).
46. G. L. Closs and J. R. Miller, *Science* **240**, 440 (1988); D. S. Wuttke, M. J. Bjerrum, J. R. Winkler, H. B. Gray, *ibid.* **256**, 1007 (1992); C. C. Moser, J. M. Keske, K. Warncke, R. S. Farid, P. L. Dutton, *Nature* **355**, 796 (1992); R. Langen *et al.*, *Science* **268**, 1733 (1995); G. M. Ullmann and N. M. Kostic, *J. Am. Chem. Soc.* **117**, 4766 (1995).
47. D. Dee and M. E. Baur, *J. Chem. Phys.* **60**, 541 (1974).
48. A. K. Felts, W. T. Pollard, R. A. Friesner, *J. Phys. Chem.* **99**, 2929 (1995); V. Mujica, M. Kemp, M. A. Ratner, *J. Chem. Phys.* **101**, 6856 (1994); *ibid.*, p. 6849; M. Kemp, V. Mujica, M. A. Ratner, *ibid.*, p. 5172.
49. Several authors have determined thermodynamic parameters for the DNA bases, but no consensus has yet emerged. See S. Steenken, J. P. Telo, H. M. Novais, L. P. Candeias, *J. Am. Chem. Soc.* **114**, 4701 (1992); N. S. Hush and A. S. Cheung, *Chem. Phys. Lett.* **34**, 11 (1975); M. Faraggi and M. H. Klapper, *J. Chim. Phys.* **91**, 1054 (1994); S. V. Jovanovic and M. G. Simic, *J. Phys. Chem.* **90**, 974 (1986); L. Kittler, G. Löber, F. A. Gollnick, H. Berg, *J. Electroanal. Chem.* **116**, 503 (1980).
50. L. A. Lipscomb *et al.*, *Biochemistry* **35**, 2818 (1996).
51. Transient absorption data on the nanosecond time scale were obtained with instrumentation described by M. Bacharach [thesis, California Institute of Technology (1995)] at concentrations of 67 μmM Ru and 3.4 mM DNA bp.
52. We are grateful to NIH (GM49216 to J.K.B.) and NSF (CHE-9304373 to P.F.B.) for financial support. We also thank NSF for predoctoral support of M.R.A. and R.E.H., and the American Cancer Society for postdoctoral support of E.D.A.S. We are also grateful to N. J. Turro for helpful discussions and to the reviewers for thoughtful comments.

22 November 1995; accepted 6 May 1996

Low-Frequency Raman Scattering and the Fast Relaxation Process in Glycerol

Takashi Uchino* and Toshinobu Yoko

Ab initio molecular orbital calculations were used to determine the structure and vibrational frequencies of the cyclic glycerol trimer, which represents the region of medium-range ordering in liquid and supercooled glycerol. The calculations reproduced the experimentally observed low-frequency Raman scattering peak (or the "boson peak") at ~50 per centimeter, which suggests that the peak results from the localized collective motions of the cooperatively hydrogen-bonded hydroxyl groups. The calculations also suggest that the fast relaxation process may result from the translational motion of each glycerol molecule in the cyclic structure. On the basis of these results, a model of the glass transition was developed.

The low-frequency (<~100 cm^{-1}) relaxations and vibrations in amorphous systems have been the focus of numerous studies aimed at understanding the anomalous low-temperature properties and glass transition phenomena observed in such systems (*1*). Although the relaxational part of the dynamics in supercooled liquids is well described by the mode coupling theory (MCT) (*2*), the vibrational excitations, generally called the "boson peak," cannot be explained in terms of MCT, and the origin of the boson peak is still unsettled. Thus, understanding the boson peak and the fast relaxation process near the glass transition temperature T_g remains an important goal in solid-state physics. It has recently been suggested that the atomic motions in a medium-range scale on the order of ~10 Å in amorphous solids are closely related to the boson peak (*3*). This hypothesis strongly suggests that the normal-mode analysis of molecules modeling a medium-range order (MRO) in a particular glass will shed light on the physical origin of the boson peak.

Glycerol has been widely used to investigate the low-frequency vibrational properties of liquids and supercooled liquids, because liquid glycerol is one of few systems that remain in the metastable supercooled state long enough to permit Raman scattering (*4–8*) and neutron scattering (*7*, *9*) measurements. The low-frequency Raman scattering spectra of glycerol below T_g (186 K) are characterized by a nonsymmetric boson peak with a broad maximum around 50 cm^{-1}; the peak shifts slightly to higher frequencies with decreasing temperature. Raman scattering measurements in the O–H stretching region have demonstrated that liquid and supercooled glycerol are self-associated through intermolecular hydrogen bonds to form dimer, trimer, and oligomer structures (*8*). Neutron diffraction measurements (*9*) have demonstrated that liquid glycerol not only has intramolecular correlations but also exhibits some residual structure in the intermediate range (2 to 6 Å). These findings indicate that, despite the flexibility of each molecular unit, the intermolecular distribution function exhibits significant structural ordering as a result of intermolecular hydrogen bonding.

Although the exact intermolecular conformation of the MRO in glycerol has not been determined, it has been demonstrated that small water (*10*) and methanol (*11*, *12*) clusters tend to form cyclic hydrogen-bonded trimers. The intermolecular hydrogen bonds in such trimers are considered to be enhanced by cooperative

Institute for Chemical Research, Kyoto University, Uji, Kyoto 611, Japan.

*To whom correspondence should be addressed.